

Stable diplatinum complexes with functional thiolato bridges from dialkylation of $[\text{Pt}_2(\mu\text{-S})_2(\text{P-P})_2]$ [$\text{P-P} = 2 \times \text{PPh}_3, \text{Ph}_2\text{P}(\text{CH}_2)_3\text{PPh}_2$] \dagger

Siew Huay Chong,^a William Henderson^b and T. S. Andy Hor^{*a}

Received 18th May 2007, Accepted 11th July 2007

First published as an Advance Article on the web 2nd August 2007

DOI: 10.1039/b707526j

The normally robust monoalkylated complexes $[\text{Pt}_2(\mu\text{-S})(\mu\text{-SR})(\text{PPh}_3)_4]^+$ can be activated towards further alkylation. Dialkylated complexes $[\text{Pt}_2(\mu\text{-SR})_2(\text{P-P})_2]^{2+}$ ($\text{P-P} = 2 \times \text{PPh}_3, \text{Ph}_2\text{P}(\text{CH}_2)_3\text{PPh}_2$) can be stabilized and isolated by the use of electron-rich and aromatic halogenated substituents R [e.g. 3-(2-bromoethyl)indole and 2-bromo-4'-phenylacetophenone] and 1,3-bis(diphenylphosphino)propane [$\text{Ph}_2\text{P}(\text{CH}_2)_3\text{PPh}_2$ or dpppp] which enhances the nucleophilicity of the $\{\text{Pt}_2(\mu\text{-S})_2\}$ core. This strategy led to the activation of $[\text{Pt}_2(\mu\text{-S})(\mu\text{-SR})(\text{PPh}_3)_4]^+$ towards R-X as well as isolation and crystallographic elucidation of $[\text{Pt}_2(\mu\text{-SC}_{10}\text{H}_{10}\text{N})_2(\text{PPh}_3)_4](\text{PF}_6)_2$ (**2a**), $[\text{Pt}_2(\mu\text{-SCH}_2\text{C}(\text{O})\text{C}_6\text{H}_4\text{C}_6\text{H}_5)_2(\text{PPh}_3)_4](\text{PF}_6)_2$ (**2b**), and a range of functionalized-thiolato bridged complexes such as $[\text{Pt}_2(\mu\text{-SR})_2(\text{dpppp})_2](\text{PF}_6)_2$ [R = $-\text{CH}_2\text{C}_6\text{H}_5$ (**8a**), $-\text{CH}_2\text{CHCH}_2$ (**8b**) and $-\text{CH}_2\text{CN}$ (**8c**)]. The stepwise alkylation process is conveniently monitored by Electrospray Ionisation Mass Spectrometry, allowing for a direct qualitative comparison of the nucleophilicity of $[\text{Pt}_2(\mu\text{-S})_2(\text{P-P})_2]$, thereby guiding the bench-top synthesis of some products observed spectroscopically.

Introduction

The “butterfly-look-alike” metalloligand $[\text{Pt}_2(\mu\text{-S})_2(\text{PPh}_3)_4]$ (**1**) is best known as a precursor to multimetallic materials.¹ Recently, there has been an emerging interest in its applied coordination chemistry as a magnet for organic electrophiles,² activation of robust C-X bonds,³ and as a templating agent for organochalcogen compounds such as dithiacyclophane,⁴ etc. Underpinning these applications lies a versatile strategy—transformation of $[\text{Pt}_2\text{S}_2]$ to $[\text{Pt}_2(\text{SR})_2]^{2+}$ via $[\text{Pt}_2(\text{S})(\text{SR})]^+$ with R being an organic moiety or metalloorganic fragment. This seemingly trivial conversion, especially towards organic nucleophiles, is plagued with problems due to the poor affinity of cationic (and electrophilic) $[\text{Pt}_2(\mu\text{-S})(\mu\text{-SR})]^+$ towards another electrophile RX. The tendency for a dicationic complex $[\text{Pt}_2(\mu\text{-SR})_2(\text{PR}_3)_4]^{2+}2\text{X}^-$ to disintegrate into two mononuclear components *viz.* $[\text{Pt}(\text{SR})_2(\text{PR}_3)_2]$ and $[\text{PtX}_2(\text{PR}_3)_2]$ is also thermodynamically overwhelming. This problem is also associated with the misinterpretation of $[\text{Pt}_2(\mu\text{-SMe})_2(\text{PPh}_3)_4]^{2+}2\text{I}^-$ from the reaction of **1** and MeI, which was later identified as $[\text{Pt}_2(\mu\text{-S})(\mu\text{-SMe})(\text{PPh}_3)_4]^+\text{I}^-$.⁵

It is therefore not surprising that amidst the large array of $[\text{Pt}_2\text{S}_2]$ -based complexes and aggregates known, there are very few doubly bridged thiolato complexes which have been prepared by dialkylation of **1**, with the exception of $[\text{Pt}_2(\mu\text{-SCH}_3)_2(\text{PPh}_3)_4](\text{PF}_6)_2$ which has recently been reported by our group.^{2a} Some have been identified under Electrospray Ionisation Mass Spectrometry (ESI-MS) conditions⁶ but they have not been synthesized as laboratory-scale products. For those that

have been isolated and structurally identified, they are assisted by the use of an overhead spacer R-R across the S...S bridge, such as $[\text{Pt}_2(\mu\text{-SC}_n\text{H}_{2n}\text{S})(\text{PPh}_3)_4](\text{PF}_6)_2$ ($n = 2$ and 4) and $[\text{Pt}_2(\mu\text{-SCH}_2\text{C}_6\text{H}_4\text{CH}_2\text{S})(\text{P-P})_2](\text{PF}_6)_2$ [$\text{P-P} = 2 \times \text{PPh}_3$ and $\text{Ph}_2\text{P}(\text{CH}_2)_3\text{PPh}_2$ (dpppp)].^{4,7} In this paper, we shall present some new findings on the activation of the monoalkylated complexes, the synthetic approach to “unsupported” doubly bridged thiolato complexes of Pt(II), and describe the conditions under which they can be stabilized and isolated.

Results and discussion

Reactivity of $[\text{Pt}_2(\mu\text{-S})_2(\text{PPh}_3)_4]$ (**1**) towards halides containing aromatic and electron-rich substituents—syntheses of dialkylated $[\text{Pt}_2(\mu\text{-SR})_2(\text{PPh}_3)_4]^{2+}$ products

The dimethylation of $[\text{Pt}_2(\mu\text{-S})_2(\text{PPh}_3)_4]$ (**1**) with dimethyl sulfate (Me_2SO_4)^{2a} to give $[\text{Pt}_2(\mu\text{-SCH}_3)_2(\text{PPh}_3)_4](\text{PF}_6)_2$ is the first example of a double-alkylation reaction on the $\{\text{Pt}_2(\mu\text{-S})_2\}$ system, giving $[\text{Pt}_2(\mu\text{-SR})_2(\text{PPh}_3)_4]^{2+}$ (**2**) with doubly bridging thiolates. The diprotonated derivative $[\text{Pt}_2(\mu\text{-SH})_2(\text{PPh}_3)_4]^{2+}$ is detected by mass spectrometry (ESI-MS),⁸ although detailed protonation studies on $[\text{Pt}_2(\mu\text{-SH})_2(\text{Ph}_2\text{P}(\text{CH}_2)_n\text{PPh}_2)_2]$ ($n = 2$ or 3) by González-Duarte *et al.*⁹ have shown that such diprotonated species are unstable in solution. However, the selenide analogue $[\text{Pt}_2(\mu\text{-SeH})_2(\text{PPh}_3)_4][\text{ClO}_4]_2$ has been isolated and crystallographically characterized.¹⁰ Attempts to prepare complexes **2** with excess monohalide, RX is hindered by the deactivation of the unsubstituted sulfide in $[\text{Pt}_2(\mu\text{-S})(\mu\text{-SR})(\text{PPh}_3)_4]^+$ (**3**) due to the positive charge on the monocation. This is exemplified in the reaction of **1** with 3-bromopropionitrile and ethyl 3-bromopropionate, which results in the rapid and exclusive formation of $[\text{Pt}_2(\mu\text{-S})(\mu\text{-SCH}_2\text{CH}_2\text{CN})(\text{PPh}_3)_4]^+$ (**3a**) and $[\text{Pt}_2(\mu\text{-S})(\mu\text{-SC}_2\text{H}_4\text{CO}_2\text{CH}_2\text{CH}_3)(\text{PPh}_3)_4]^+$ (**3b**), respectively. Both **3a** and **3b** remain stable to further alkylation even in the presence of excess

^aDepartment of Chemistry, National University of Singapore, 3, Science Drive 3, Singapore, 117543, Singapore. E-mail: andyhor@nus.edu.sg; Fax: +(65) 6873 1324; Tel: +(65) 6874 2663

^bDepartment of Chemistry, University of Waikato, Private Bag 3105, Hamilton, New Zealand

\dagger CCDC reference numbers 647935–647939. For crystallographic data in CIF or other electronic format see DOI: 10.1039/b707526j

alkyl halides. Single-crystal X-ray diffraction analyses of the PF₆ salt of **3a** and **3b** confirmed the presence of mixed thiolate–sulfide bridges (Fig. 1). The {Pt₂(μ-S)₂} butterflies of both structures are inevitably bent with dihedral angles (θ) between the two PtS₂ planes of 144° (**3a**) and 157° (**3b**), compared with 168° in the parent complex **1**.¹¹ A larger degree of bending is expected in order to accommodate the bridge substituent and minimize its repulsion with the terminal PPh₃. Alkylation of the sulfide bridges lengthens the Pt–S bond, as evidenced in the longer Pt–SCH₂CH₂CN (Pt(2)–S(1) = 2.3525 Å) length relative to that of Pt–S (Pt(2)–S(2) = 2.345 Å). The thiolate ligand adopts an *exo* conformation, pointing away from the bulky triphenylphosphines. Noticeably, the thiolate ligand in **3a** appears to hover above the unsubstituted sulfide thus causing steric hindrance. This could provide another explanation for the resistance of the unsubstituted sulfide towards further alkylation. An ESI-MS study using weak monofunctional alkylating agents⁶ such as *n*-butyl chloride, Me₂NCH₂CH₂Cl·HCl, bromoethylphthalimide, PhNHCOCH₂Cl, and hydrazones such as PhC(=NNHAr)CH₂Br and CH₃C(=NNHAr)CH₂Cl, all pointed to selective monoalkylation of the {Pt₂(μ-S)₂} core.

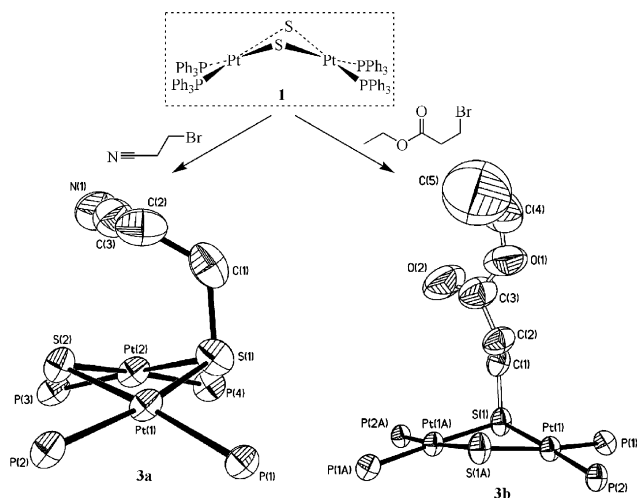


Fig. 1 50% thermal ellipsoid representation of the cations of [Pt₂(μ-S)(μ-SCH₂CH₂CN)(PPh₃)₄](PF₆) (**3a**) and [Pt₂(μ-S)(μ-SC₂H₄CO₂CH₂CH₃)(PPh₃)₄](PF₆) (**3b**). The phenyl rings of PPh₃ and hydrogen atoms are omitted for clarity.

Further alkylation of **3** can be achieved by using a powerful methylating agent (Me₂SO₄) to give the mixed thiolato bridging complex [Pt₂(μ-SR)(μ-SCH₃)(PPh₃)₄]²⁺ [R = –CH₂C₆H₅, –CH₂CHCH₂, –C₃H₁₀CO₂CH₂CH₃, –C₂H₄CO₂CH₂CH₃, –CH₂CH₂CN, –C₂H₄CH(O)₂C₂H₄ and –C₂H₄SC₆H₅]. This is however limited to the introduction of the methyl substituent.^{2a} General dialkylation of **1** to [Pt₂(μ-SR)₂(PPh₃)₄]²⁺ (**2**) is achieved by the choice of an appropriate alkylating agent.⁶ Reactive alkyl halides such as allyl bromide and methyl chloroacetate lead to the stepwise formation of [Pt₂(μ-SCH₂CHCH₂)₂(PPh₃)₄]²⁺ and [Pt₂(μ-SCH₂CO₂CH₃)₂(PPh₃)₄]²⁺ upon prolonged reactions. Reactive halides that contain aromatic and electron-rich substituents generally give successful reactions. This is also demonstrated by the use of 3-(2-bromoethyl)indole, which is an aromatic, heterocyclic compound with a highly electron delocalized structure at the fused rings (fused benzene and pyrrole). When the

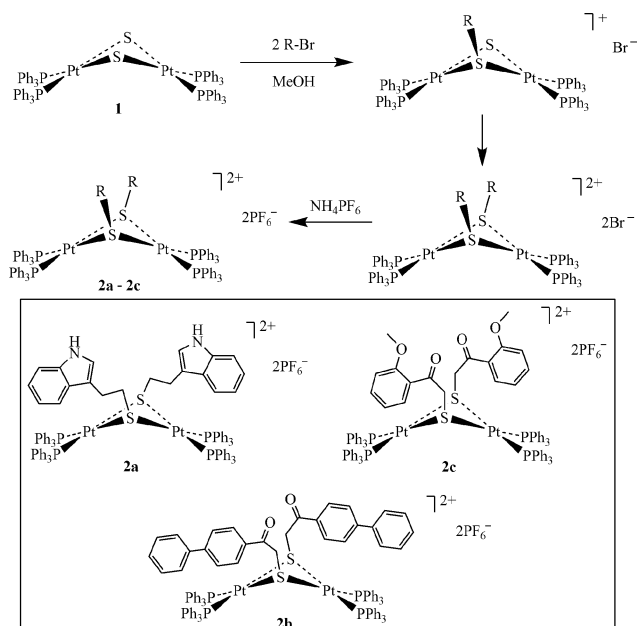
Table 1 Principal ions observed in the ESI-MS-monitored reactions of [Pt₂(μ-S)₂(PPh₃)₄] (**1**) with reactive monoalkylating halides

Alkylating agents	Reaction time ^a	Observed ions (<i>m/z</i> , %)
	1 h	3c (1647, 100), 2a (896, 45)
	3 h	2a (896, 100), 3c (1647, 10)
	1 d	2a (895, 100)
	1 h	2b (946, 100)
	1 d	2b (946, 100), 4 (1711, 19)
	1 h	3d (1651, 100), 2c (901, 10)
	3 d	3d (1651, 100), 2c (900, 86)
	1 week	2c (900, 100), 3d (1652, 33)

^a Refers to the reaction time at which an aliquot from the reaction mixture is analyzed by ESI-MS.

reaction of **1** with 3-(2-bromoethyl)indole is monitored by ESI-MS, (Table 1) it clearly demonstrates a stepwise alkylation from the first hour of reaction and that both sulfur sites are susceptible to attack, as evidenced by the peaks [Pt₂(μ-S)(μ-SC₁₀H₁₀N)(PPh₃)₄]⁺ (**3c**) (*m/z* 1647, 100%) and [Pt₂(μ-SC₁₀H₁₀N)₂(PPh₃)₄]²⁺ (**2a**) (*m/z* 896, 45%). The dialkylated **2a** becomes the predominant species after 3 h of reaction and **3c** is barely noticeable in the ESI mass spectrum, suggesting complete dialkylation. Likewise, the reaction of **1** with a similar substrate, that is, 2-bromo-4'-phenylacetophenone (BrCH₂C(O)C₆H₄C₆H₅), a halide that possesses aromatic (biphenyl), π-conjugated functionalities, results in dialkylation, which proceeds to completion within an hour to give [Pt₂(μ-SCH₂C(O)C₆H₄C₆H₅)₂(PPh₃)₄]²⁺ (**2b**) (*m/z* 946, 100%). The monoalkylated species, [Pt₂(μ-S)(μ-SCH₂C(O)C₆H₄C₆H₅)(PPh₃)₄]⁺ is absent in the mass spectrum, pointing to a faster rate of reaction. Not only does the ESI-MS provide a simple technique to follow the course of reaction, it also identifies the formation of possible side product(s). This is illustrated by the identification of a phosphine-displaced complex [Pt₂(μ-SCH₂C(O)C₆H₄C₆H₅)(PPh₃)₃Br]⁺ (**4**) (*m/z* 1711, 19%) after 1 d of reaction.

The stability of novel complexes **2a** and **2b** may be enhanced by the π–π interaction between the two sets of aromatic substituents on each bridging sulfide. When an alkyl halide containing less aromatic substituents is used, such as 2-bromo-2'-methoxyacetophenone, BrCH₂C(O)C₆H₄(OCH₃), the tendency for dialkylation is noticeably lower. Under such circumstances, the monoalkylated species, [Pt₂(μ-S)(μ-SCH₂C(O)C₆H₄(OCH₃))(PPh₃)₄]⁺ (**3d**) (*m/z* 1651, 100%) becomes the predominant species, even after 3 d of reaction. Although the dialkylated product [Pt₂(μ-SCH₂C(O)C₆H₄(OCH₃)₂(PPh₃)₄]²⁺ (**2c**) (*m/z* 901, 10%) starts to form in the first hour, it becomes the major product (*m/z* 900, 100%) after 1 week. The complex **3d** (*m/z* 1652, 33%) however remains present, as observed in the mass spectrum, thus demonstrating incomplete dialkylation. Scheme 1 summarizes the reaction of **1** with these reactive halides.



Scheme 1 Dialkylation reactions of $[\text{Pt}_2(\mu\text{-S})_2(\text{PPh}_3)_4]$ (**1**) with reactive halides containing aromatic, electron-rich substituents.

We have reported earlier the synthetic applications of ESI-MS.^{6,12} This is also applicable to the successful syntheses of both diplatinum bis(μ -thiolate) complexes as the PF_6 salts, *i.e.* $[\text{Pt}_2(\mu\text{-SC}_{10}\text{H}_{10}\text{N})_2(\text{PPh}_3)_4](\text{PF}_6)_2$ (**2a**) and $[\text{Pt}_2(\mu\text{-SCH}_2\text{C}(\text{O})\text{C}_6\text{H}_4\text{C}_6\text{H}_5)_2(\text{PPh}_3)_4](\text{PF}_6)_2$ (**2b**) in good isolated yields (90% and 98%, respectively). The single crystal X-ray diffraction analysis of complex **2a** (Fig. 2) shows the two indole-substituted thiolate bridging ligands in a *syn-exo* conformation, pointing away from the sterically bulky PPh_3 ligands. The two aromatic (fused benzene and pyrrole) rings are oriented perpendicular to each other, and separated at a distance where steric repulsion is averted. The complex has a C_2 symmetry at the molecular centre, with a bent $\{\text{Pt}_2(\mu\text{-S})_2\}$ ring hinged at a dihedral angle of 140° , which is similar to that observed in mono- and other dialkylated complexes. The extent of hinging in the $\{\text{Pt}_2(\mu\text{-S})_2\}$ ring seems to be

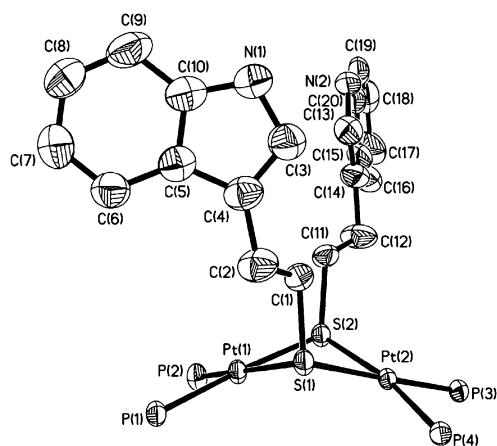


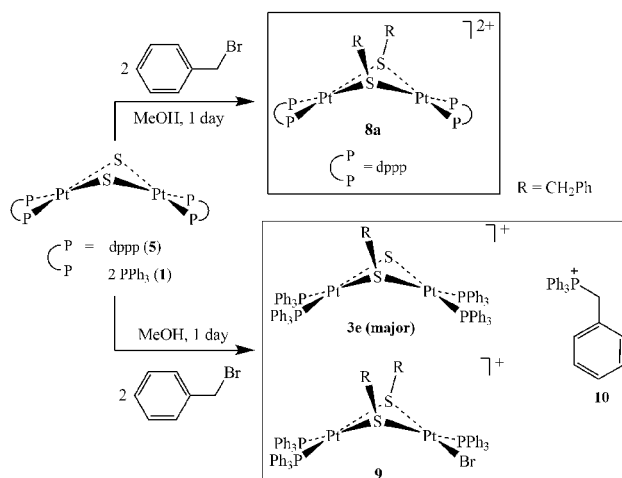
Fig. 2 A 50% thermal ellipsoid representation of the cation of $[\text{Pt}_2(\mu\text{-SC}_{10}\text{H}_{10}\text{N})_2(\text{PPh}_3)_4](\text{PF}_6)_2$ (**2a**). The phenyl rings of PPh_3 and hydrogen atoms are omitted for clarity.

unaffected by the variation and degree of functionalization about the sulfur bridges. The $^{31}\text{P}\{^1\text{H}\}$ NMR spectrum of **2a** is consistent with the symmetrical nature of the molecule, displaying a singlet at $\delta_{\text{p}} = 19.6$ ppm with the associated satellites, $^1J_{\text{Pt-P}} = 2926$ Hz for all the chemically equivalent phosphine groups. Similar $^{31}\text{P}\{^1\text{H}\}$ NMR characteristics are observed in complex **2b**—a singlet is observed at $\delta_{\text{p}} = 20.0$ ppm ($^1J_{\text{Pt-P}} = 3117$ Hz). The stronger Pt–P coupling in **2b** is consistent with a higher electronegativity or greater share of electron density in its π -conjugated biphenyl structure, which also supports a faster dialkylation of **1** with 2-bromo-4'-phenylacetophenone.

Enhancing the nucleophilicity of $\{\text{Pt}_2(\mu\text{-S})_2\}$ by replacing terminal PPh_3 with chelating $\text{Ph}_2\text{P}(\text{CH}_2)_n\text{PPh}_2$ ligands—syntheses of dialkylated $[\text{Pt}_2(\mu\text{-SR})_2(\text{dppp})_2]^{2+}$ products

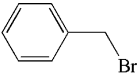
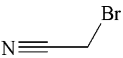
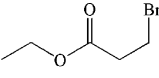
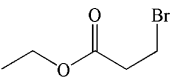
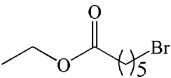
In a study of the reaction of $[\text{Pt}_2(\mu\text{-S})_2(\text{Ph}_2\text{P}(\text{CH}_2)_n\text{PPh}_2)_2]$ [$n = 3$, dppp (**5**); $n = 2$, dppe (**6**)] in CH_2Cl_2 , it is shown that nucleophilic behaviour is highly dependent on the nature of the phosphines.^{3a} The complex $[\text{Pt}_2(\mu\text{-S})_2(\text{dppp})_2]$ (**5**) is expected to be more basic than **1** because the more efficient electron donation of dppp should render the *trans*-sulfide more electron-rich and nucleophilic. The lower steric demand of dppp compared to $2 \times \text{PPh}_3$ is also expected to provide more room for the incoming electrophile. The sulfide in **5** could provide a more facile route to the second alkylation and hence formation of dithiolato bridges even with the use of simple monohalides. Formation of $[\text{Pt}_2(\mu\text{-SR})_2(\text{dppp})_2]^{2+}$ (**8**) from **5** through $[\text{Pt}_2(\mu\text{-S})(\mu\text{-SR})(\text{dppp})_2]^+$ (**7**) is therefore expected to occur.

Indeed, when **5** and **1** are compared directly (ESI-MS) in their reactions with benzyl bromide, the higher reactivity of the former is immediately evident from the clean formation of the dibenzylated, $[\text{Pt}_2(\mu\text{-SCH}_2\text{C}_6\text{H}_5)_2(\text{dppp})_2]^{2+}$ (**8a**) (m/z 731, 100%) within 1 d of reaction (Scheme 2). Similar reaction with **1** proceeds much slower over 2 d and gives $[\text{Pt}_2(\mu\text{-S})(\mu\text{-SCH}_2\text{C}_6\text{H}_5)(\text{PPh}_3)_4]^+$ (**3e**) as the major species, and the dialkylated product being the minor species.



Scheme 2 Comparison of the reaction rates of complexes **1** and **5** with benzyl bromide. A faster reaction rate is observed when the dppp ligand is used in place of PPh_3 . Dialkylation is completed in the reaction of **5** while the monoalkylated $[\text{Pt}_2(\mu\text{-S})(\mu\text{-SCH}_2\text{C}_6\text{H}_5)(\text{PPh}_3)_4]^+$ (**3e**) remains as the major species in the reaction of **1**.

Table 2 Ionic species observed in the ESI-MS-monitored reactions of $[\text{Pt}_2(\mu\text{-S})_2(\text{dppp})_2]$ (**5**) with monoalkylating halides.

Alkylating agent	Reaction time ^a and conditions	Observed ions (<i>m/z</i> , %)
	1 d	$[\text{Pt}_2(\mu\text{-SCH}_2\text{C}_6\text{H}_5)_2(\text{dppp})_2]^{2+}$ (8a) (731, 100); $[\text{Pt}_2(\mu\text{-SCH}_2\text{C}_6\text{H}_5)_2(\text{dppp})_2]^{2+}\text{Br}^-$ (1541, 28)
	1 h	$[\text{Pt}_2(\mu\text{-SCH}_2\text{CHCH}_2)_2(\text{dppp})_2]^{2+}$ (8b) (681, 100); $[\text{Pt}_2(\mu\text{-S})(\mu\text{-SCH}_2\text{CHCH}_2)(\text{dppp})_2]^+$ (7b) (1319, 25); $[\text{Pt}_2(\mu\text{-SCH}_2\text{CHCH}_2)_2(\text{dppp})_2]^{2+}\text{Br}^-$ (1440, 10)
	5 h	8b (680.5, 100); $[\text{Pt}_2(\mu\text{-SCH}_2\text{CHCH}_2)_2(\text{dppp})_2]^{2+}\text{Br}^-$ (1440, 17)
	1 h	$[\text{Pt}_2(\mu\text{-SCH}_2\text{CN})_2(\text{dppp})_2]^{2+}$ (8c) (679, 100); $[\text{Pt}_2(\mu\text{-SCH}_2\text{CN})_2(\text{dppp})_2]^{2+}\text{Br}^-$ (1439, 45)
	4 h	$[\text{Pt}_2(\mu\text{-S})(\mu\text{-SC}_2\text{H}_4\text{CO}_2\text{CH}_2\text{CH}_3)(\text{dppp})_2]^+$ (7d) (1379, 100); $[\text{Pt}_2(\mu\text{-SC}_2\text{H}_4\text{CO}_2\text{CH}_2\text{CH}_3)_2(\text{dppp})_2]^{2+}$ (8d) (740, 29)
	1 d	8d (740, 100); 7d (1379, 65); $[\text{Pt}_2(\mu\text{-SC}_2\text{H}_4\text{CO}_2\text{CH}_2\text{CH}_3)_2(\text{dppp})_2]^{2+}\text{Br}^-$ (1560, 10)
	4 d	8d (740, 100); 7d (1379, 9); $[\text{Pt}_2(\mu\text{-SC}_2\text{H}_4\text{CO}_2\text{CH}_2\text{CH}_3)_2(\text{dppp})_2]^{2+}\text{Br}^-$ (1561, 24)
	1 week	8d (740, 100)
	1 h, 60 °C	7d (1380, 100); 8d (740, 16)
	1 d, 60 °C	8d (740, 100); 7d (1379, 30); $[\text{Pt}_2(\mu\text{-SC}_2\text{H}_4\text{CO}_2\text{CH}_2\text{CH}_3)_2(\text{dppp})_2]^{2+}\text{Br}^-$ (1560, 26)
	2 d, 60 °C	8d (740, 100); 7d (1380, 5); $[\text{Pt}_2(\mu\text{-SC}_2\text{H}_4\text{CO}_2\text{CH}_2\text{CH}_3)_2(\text{dppp})_2]^{2+}\text{Br}^-$ (1561, 30)
	5 h	$[\text{Pt}_2(\mu\text{-S})(\mu\text{-SC}_5\text{H}_{10}\text{CO}_2\text{CH}_2\text{CH}_3)(\text{dppp})_2]^+$ (7e) (1421, 100); $[\text{Pt}_2(\mu\text{-SC}_5\text{H}_{10}\text{CO}_2\text{CH}_2\text{CH}_3)_2(\text{dppp})_2]^{2+}$ (8e) (783, 8)
	1 d	7e (1421, 100); 8e (782, 45)
	3 d and 60 °C for 2 d	8e (782, 100); $[\text{Pt}_2(\mu\text{-SC}_5\text{H}_{10}\text{CO}_2\text{CH}_2\text{CH}_3)_2(\text{dppp})_2]^{2+}\text{Br}^-$ (1645, 46)

^a Refers to the reaction time at which an aliquot from the reaction mixture is analyzed by ESI-MS.

Other side products, such as $[\text{Pt}_2(\mu\text{-SCH}_2\text{C}_6\text{H}_5)_2(\text{PPh}_3)\text{Br}]^+$ (**9**) and the phosphonium ion $[\text{Ph}_3\text{PCH}_2\text{C}_6\text{H}_5]^+$ (**10**) are also observed. Use of dppp also suppresses the problem of phosphine displacement (as in **9**). Reactions towards other monohalides give similar conclusions. The ESI-MS data are summarized in Table 2.

The complex $[\text{Pt}_2(\mu\text{-SCH}_2\text{C}_6\text{H}_5)_2(\text{dppp})_2](\text{PF}_6)_2$ **8a**, isolated in 81% yield, represents the first isolated doubly-bridged dithiolato complex $[\text{Pt}_2(\mu\text{-SR})_2(\text{dppp})_2]^{2+}$ arising from alkylation of **5**. The related diprotonated species, $[\text{Pt}_2(\mu\text{-SH})_2(\text{dppp})_2]^{2+}$ is unstable in solution and decomposes to mononuclear complexes.⁹ The $^1\text{P}\{^1\text{H}\}$ NMR spectrum of **8a** is typical of a symmetrical structure and displays a singlet at $\delta_{\text{p}} = -0.7$ ppm with the associated satellites for the Pt–P coupling, $^1J_{\text{Pt-P}} = 2733$ Hz for the chemically equivalent phosphine groups. Confirmation of its identity by an X-ray diffraction study (Fig. 3) also shows that the two benzyl thiolate ligands adopt a *syn-exo* conformation, pointing away from the diphosphines. The central $\{\text{Pt}_2(\mu\text{-S})_2\}$ ring is hinged with a dihedral angle of 141° , a modest increase from the parent complex, **5** ($\theta = 135^\circ$),^{3a} accompanied by a slight lengthening of the Pt...Pt distance to 3.333 Å (from 3.235 Å in **5**). It is worth pointing out that although **5** reacts with CH_2Cl_2 ^{3a} and protic acid⁸ leading to fragmentation of the $\{\text{Pt}_2(\mu\text{-SR})_2\}$ core, examination of the Pt–S bonds in **8a** gives no indication that the Pt–S bonds are weakened by the dialkylation. A comparison with the molecular structure of $[\text{Pt}_2(\mu\text{-S})(\mu\text{-SCH}_2\text{C}_6\text{H}_5)(\text{PPh}_3)_4](\text{PF}_6)$ (**3e**) (Fig. 4) is made: the Pt–S(CH₂C₆H₅) bond lengths in the monoalkylated **3e** (Pt(1)–S(1) = 2.3667(13) Å) and dibenzylated, **8a** (Pt(1)–S(1) = 2.370(3) Å and Pt(1)–S(2) = 2.372(3) Å) are comparable. This

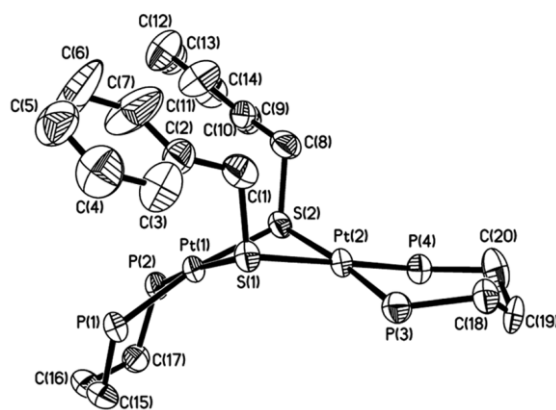


Fig. 3 A 50% thermal ellipsoid representation of the cation of $[\text{Pt}_2(\mu\text{-SCH}_2\text{C}_6\text{H}_5)_2(\text{dppp})_2](\text{PF}_6)_2$ (**8a**). The phenyl rings of dppp and hydrogen atoms are omitted for clarity.

suggests that the stability of the dialkylated products depend not only on the peripheral phosphine or the basicity of the counter anion, but also the nature of the alkyl substituent.

Successful reactions have also been achieved with allyl bromide, bromoacetonitrile, ethyl 3-bromopropionate and ethyl 6-bromohexanoate, resulting in the formation of $[\text{Pt}_2(\mu\text{-SCH}_2\text{CHCH}_2)_2(\text{dppp})_2]^{2+}$ (**8b**) (*m/z* 680.5, 100%), $[\text{Pt}_2(\mu\text{-SCH}_2\text{CN})_2(\text{dppp})_2]^{2+}$ (**8c**) (*m/z* 679, 100%), $[\text{Pt}_2(\mu\text{-SC}_2\text{H}_4\text{CO}_2\text{CH}_2\text{CH}_3)_2(\text{dppp})_2]^{2+}$ (**8d**) (*m/z* 740, 100%) and $[\text{Pt}_2(\mu\text{-SC}_5\text{H}_{10}\text{CO}_2\text{CH}_2\text{CH}_3)_2(\text{dppp})_2]^{2+}$ (**8e**) (*m/z* 782, 100%), respectively. As before, the chelating effect

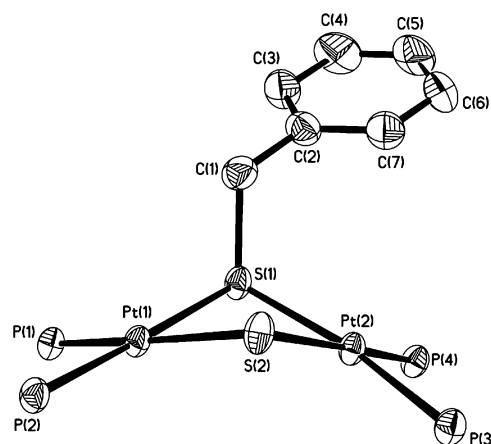
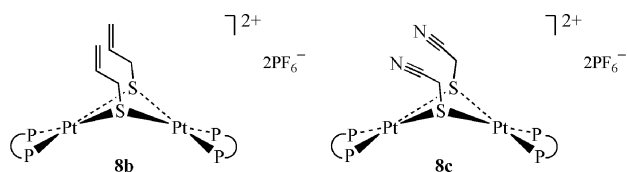


Fig. 4 A 50% thermal ellipsoid representation of the cation of $[\text{Pt}_2(\mu\text{-S})(\mu\text{-SCH}_2\text{C}_6\text{H}_5)(\text{PPh}_3)_4](\text{PF}_6)$ (**3e**). The phenyl rings of PPh_3 and hydrogen atoms are omitted for clarity.

of dppp helps to preserve the phosphine and protect it from displacement by free bromide (Table 2). The free bromide, however, appears in an ion pair with the dialkylated $[\text{Pt}_2(\mu\text{-SR})_2(\text{dppp})_2]^{2+}$ complexes giving $[\{\text{Pt}_2(\mu\text{-SR})_2(\text{dppp})_2\}\text{Br}]^+$. Reaction with bromoacetonitrile proceeds with completion almost immediately (within an hour at r.t.) to give the dialkylated species as the sole product. The other reactions are slower, such that the stepwise alkylation can be followed by ESI-MS changes. While the reaction with allyl bromide is completed in 5 h at r.t., those with longer chain halides containing ester functionalities are slower and require heating at approximately 60°C for 2 d in order for dialkylation to be complete. Preparation of the ESI mass spectrometrically observed species is straightforward and results in reasonably good yields, which is illustrated in the preparation of the dialkylated complexes, $[\text{Pt}_2(\mu\text{-SCH}_2\text{CHCH}_2)_2(\text{dppp})_2](\text{PF}_6)_2$ (**8b**) (80% yield) and $[\text{Pt}_2(\mu\text{-SCH}_2\text{CN})_2(\text{dppp})_2](\text{PF}_6)_2$ (**8c**) (71% yield).



The use of dppp to enhance the sulfide reactivity and rate towards alkylation has an opposite effect to that used by Henderson *et al.*¹³ on AsPh_3 and González-Duarte *et al.*¹⁴ on $\text{Ph}_2\text{As}(\text{CH}_2)_2\text{AsPh}_2$ (dpae); the latter ligands tend to reduce the basicity of the $\{\text{Pt}_2(\mu\text{-S})_2\}$ core. With this knowledge, we are now in a better position to tune and control the reactivity of the sulfide bridge towards a range of Lewis acids or electrophiles and direct the product outcome, be it mono- or dithiolate formation, and tri- or tetrametallic aggregate formation.

Although alkylation of the μ -sulfido ligands is an established concept,¹⁵ it is ironic that such a seemingly straightforward and powerful reactivity has resulted in only a few synthetically useful methods in the preparation of thiolate bridged complexes. There are a few main reasons. The majority of sulfide complexes in the literature have μ_3 or capping sulfide, which has very poor nucleophilicity towards R-X . These are not suitable precursors for thiolate complexes. The μ_2 bridging sulfide is much more reactive

and suitable, but in this group, there are many more singly-bridging $[\text{M}-\mu_2\text{-S}-\text{M}]$ than doubly bridging $[\text{M}-(\mu_2\text{-S})_2-\text{M}]$ sulfides. The former tends to alkylate to give $[\text{M}-\mu_2\text{-SR}-\text{M}]^+$ but there is little tendency for a second alkylation to take place. Forceful alkylation would only lead to the collapse of the complex and release of R_2S . There is also a more facile competitive pathway—alkylation of the metal giving metal alkyls. The $\{\text{M}_2(\mu\text{-S})_2\}$ core is hence the most convenient template for dithiolato bridged complexes. Such complexes could provide an entry to other organometallic complexes.^{15a} Unfortunately, such a core is known to be highly basic and nucleophilic, and many such complexes could not be isolated. Hence the $[\text{Pt}_2(\mu\text{-S})_2(\text{PR}_3)_4]$ or $[\text{Pt}_2(\mu\text{-S})_2(\text{P-P})_2]$ series are among the very few dinuclear doubly bridging sulfide complexes that can be isolated and prepared in good yield. Its high shelf-life and resistance towards (aerial) oxidation or hydrolysis thus makes this a unique complex and a useful addition to pre-existing methodology for accessing a range of Pt sulfide-based materials.

Conclusion

We have found a simple solution to a long-standing problem. The method developed herein allows us to bypass the use of thiolato substrates¹⁶ such as $[\text{Pt}(\text{SR})_2(\text{PR}_3)_2]$ which are generally prepared from the repulsive thiols RSH or their salts.¹⁷ The alternative of using **1** or **5** as a precursor also has other advantages such as its easy preparation from cheap and readily available Na_2S by a one-pot method. Another key benefit is that the current methodology is generally applicable to a large variety of aliphatic, aromatic and heterocyclic halides. Using the mononuclear thiolato route would be problematic because this would require the subsequent preparation of the $[\text{Pt}(\text{SR})_2(\text{PR}_3)_2]$ that makes use of functional thiols that are unstable and may be difficult to access. Isolation of the complexes described suggests that we could design and incorporate different functionalities on the alkyl residue such as nitrile, ester, allyl, benzyl, indolyl and ketone, *etc.* The syntheses herein therefore could provide a pathway to functional thiolates for different applications. In addition, our method potentially paves the way to prepare hetero-dithiolated complexes, $[\text{Pt}_2(\mu\text{-SR})(\mu\text{-SR}')(\text{dppp})_2]^{2+}$ (where $\text{R} \neq \text{R}' \neq \text{CH}_3$). Details of such syntheses will be reported in due course. Our current effort is hence directed at anchoring the $\{\text{Pt}_2(\mu\text{-S})_2\}$ moiety on a solid support by thiolato spacers thus expanding the current use of thiolates in homogeneous catalysis,^{16a,18} molecular electronics,^{16b,19} and medicine,²⁰ *etc.*

Experimental

Methods and materials

All manipulations were carried out at room temperature, unless otherwise stated, under an atmosphere of nitrogen. Solvents used were generally analytical grade (Tedia), dried and deoxygenated before used. $[\text{Pt}_2(\mu\text{-S})_2(\text{PPh}_3)_4]$ (**1**) was synthesized by metathesis of *cis*- $[\text{PtCl}_2(\text{PPh}_3)_2]$ with $\text{Na}_2\text{S}\cdot 9\text{H}_2\text{O}$ (Riedel-de Haën) in benzene suspension, followed by filtration, and washing with water to remove soluble sodium salts. ESI-MS (80% MeOH–20% H_2O): m/z 1503 $[\text{M} + \text{H}^+]$. $[\text{Pt}_2(\mu\text{-S})_2(\text{dppp})_2]$ (**5**) was synthesized according to published methods.^{3a} ESI-MS (80% MeOH–20% H_2O): m/z 1279 $[\text{M} + \text{H}^+]$. The following chemicals were used as

supplied from Aldrich: allyl bromide, benzyl bromide, bromoacetonitrile, 3-bromopropionitrile, 3-(2-bromoethyl)indole, 2-bromo-4'-phenylacetophenone, 2-bromo-2'-methoxyacetophenone, and ammonium hexafluorophosphate. Ethyl 3-bromopropionate and ethyl 6-bromohexanoate were obtained from TCI.

Elemental analyses were performed on a Perkin-Elmer PE 2400 CHNS elemental analyzer. ^1H and ^{13}C NMR spectra were recorded at 25 °C on a Bruker ACF 300 spectrometer (at 300 and 75.47 MHz, respectively) with Me_4Si as internal standard. The ^{31}P NMR spectra were recorded at 25 °C at 121.50 MHz with 85% H_3PO_4 as external reference. Electrospray mass spectra were obtained in the positive-ion mode with a Finnigan/MAT LCQ mass spectrometer coupled with a TSP4000 HPLC system and the crystal 310 CE system. The mobile phase was 80% methanol–20% H_2O (flow rate: 0.4 mL min^{-1}). The capillary temperature was 150 °C. Peaks were assigned from the m/z values and from the isotope-distribution patterns.

Syntheses

[Pt₂(μ-S)(μ-SCH₂CH₂CN)(PPh₃)₄](PF₆) (3a). 3-Bromopropionitrile (20.0 μL, 32.3 mg, 0.241 mmol, 12 equiv.) and compound **1** (29.9 mg, 0.020 mmol) in methanol (10 mL) gave a yellow solution within 10 min. After stirring for 2.25 h, excess NH_4PF_6 (15.0 mg, 0.092 mmol) was added, turning the solution into a yellow suspension. Deionized water (30 mL) was used to complete the precipitation. The yellow precipitate was washed with deionized water (100 mL) and diethyl ether (100 mL) using vacuum suction filtration to yield a bright yellow powder of **3a** (29.4 mg, 87%). $^{31}\text{P}\{^1\text{H}\}$ NMR (CDCl_3): $\delta_{\text{P}} = 24.6$ ppm (br s, $^1J_{\text{Pt-P(1)}} = 3319$ Hz, $^1J_{\text{Pt-P(2)}} = 2579$ Hz); ^1H NMR (CD_2Cl_2): $\delta_{\text{H}} = 1.80$ (t, $J = 7.5$ Hz, 2 H; CH_2CN), 1.97 (br s, 2 H; SCH_2), 7.09–7.40 ppm (m, 60 H; $12\text{C}_6\text{H}_5$); ESI-MS ($\text{MeOH-H}_2\text{O}$): m/z (%): 1557 ($[\text{M}]^+$, 100); elemental analysis: calcd (%) for $\text{Pt}_2\text{S}_2\text{C}_7\text{H}_6\text{P}_3\text{F}_6\text{N}$ (1702.47): C 52.91, H 3.80, N 0.82, S 3.77; found (%): C 52.67, H 3.65, N 0.81, S 4.04. Yellow crystals of $[\text{Pt}_2(\mu\text{-S})(\mu\text{-SCH}_2\text{CH}_2\text{CN})(\text{PPh}_3)_4](\text{PF}_6)$ suitable for X-ray crystallographic analysis were obtained from dichloromethane–methanol.

[Pt₂(μ-S)(μ-SC₂H₄CO₂CH₂CH₃)(PPh₃)₄](PF₆) (3b). Ethyl 3-bromopropionate (50.0 μL, 63.0 mg, 0.348 mmol, 10 equiv.) and compound **1** (50.8 mg, 0.034 mmol) in methanol (20 mL) gave a yellow solution after 10 min. The mixture was stirred for 2.5 h, followed by the addition of excess NH_4PF_6 (15.0 mg, 0.092 mmol), which turned the solution into a yellow suspension. Deionized water (50 mL) was used to complete the precipitation. Yellow powder of **3b** (48.4 mg, 82%) was obtained by washing with deionized water (100 mL) and diethyl ether (100 mL) using vacuum suction filtration. $^{31}\text{P}\{^1\text{H}\}$ NMR (CD_2Cl_2): $\delta_{\text{P}} = 24.7$ ppm (br s, $^1J_{\text{Pt-P(1)}} = 3280$ Hz, $^1J_{\text{Pt-P(2)}} = 2596$ Hz); ^1H NMR (CD_2Cl_2): $\delta_{\text{H}} = 1.24$ (t, $J = 7.2$ Hz, 3 H; OCH_2CH_3), 1.62 (t, $J = 8.6$ Hz, 2 H; CH_2CO), 2.35 (br s, 2 H; SCH_2), 3.98–4.06 (q, $J = 7.2$ Hz, 2 H; OCH_2), 7.06–7.43 ppm (m, 60 H; $12\text{C}_6\text{H}_5$); ESI-MS ($\text{MeOH-H}_2\text{O}$): m/z (%): 1604 ($[\text{M}]^+$, 100); elemental analysis: calcd (%) for $\text{Pt}_2\text{S}_2\text{C}_{77}\text{H}_{69}\text{P}_3\text{F}_6\text{O}_2$ (1749.52): C 52.86, H 3.98, S 3.67; found (%): C 52.78, H 3.95, S 3.54. Orange crystals of $[\text{Pt}_2(\mu\text{-S})(\mu\text{-SC}_2\text{H}_4\text{CO}_2\text{CH}_2\text{CH}_3)(\text{PPh}_3)_4](\text{PF}_6)$ suitable for X-ray crystallographic analysis were obtained from dichloromethane–methanol.

[Pt₂(μ-SC₁₀H₁₀N)₂(PPh₃)₄](PF₆)₂ (2a). 3-(2-Bromoethyl)indole (79.2 mg, 0.353 mmol, 7 equiv.) was introduced into an orange suspension of **1** (79.2 mg, 0.053 mmol) in methanol (35 mL). The mixture was stirred for 4 h to give a pale yellow solution, followed by the addition of excess NH_4PF_6 (20.0 mg, 0.123 mmol). Deionized water (70 mL) was added to induce precipitation. Pale yellow powder of **2a** (98.6 mg, 90%) was obtained after washing with water (100 mL) and diethyl ether (100 mL) using vacuum suction filtration. $^{31}\text{P}\{^1\text{H}\}$ NMR (CD_2Cl_2): $\delta_{\text{P}} = 19.6$ ppm (s, $^1J_{\text{Pt-P}} = 2926$ Hz); ^1H NMR (CD_2Cl_2): $\delta_{\text{H}} = 1.64$ –1.70 (br m, 4 H; 2SCH_2), 2.02 (br s, 4 H; $2\text{SCH}_2\text{CH}_2$), 6.53 (s, 2 H; $2\text{C}=\text{CHNH}$), 6.81–6.84 (br d, $J = 7.9$ Hz, 4 H; $2\text{C}_6\text{H}_4$), 7.00 (br t, $J = 7.1$ Hz, 4 H; $2\text{C}_6\text{H}_4$), 7.22–7.49 (m, 60 H; $12\text{C}_6\text{H}_5$), 8.62 (s, 2 H; $2\text{C}=\text{CHNH}$); ESI-MS ($\text{MeOH-H}_2\text{O}$): m/z (%): 895.5 ($[\text{M}]^{2+}$, 100), 1935 (15, $[\text{M}]^{2+}[\text{PF}_6]^-$); elemental analysis: calcd (%) for $\text{Pt}_2\text{S}_2\text{C}_{92}\text{H}_{80}\text{P}_6\text{F}_{12}\text{N}_2$ (2081.74): C 53.08, H 3.87, N 1.35, S 3.08; found (%): C 52.80, H 4.02, N 1.39, S 2.86. Pale yellow crystals of $[\text{Pt}_2(\mu\text{-SC}_{10}\text{H}_{10}\text{N})_2(\text{PPh}_3)_4](\text{PF}_6)_2$ suitable for X-ray crystallographic analysis were obtained from dichloromethane–methanol.

[Pt₂(μ-SCH₂C(O)C₆H₄C₆H₅)₂(PPh₃)₄](PF₆)₂ (2b). 2-Bromo-4'-phenylacetophenone (65.0 mg, 0.236 mmol, 6 equiv.) was introduced into an orange suspension of **1** (59.7 mg, 0.040 mmol) in methanol (22 mL). Solubilization occurred after 5 min and the dark yellow solution was left to stir overnight. Excess NH_4PF_6 (20.0 mg, 0.123 mmol) was added, resulting in a light yellow suspension. Deionized water (50 mL) was added to complete precipitation. Yellowish–orange powder of **2b** (84.8 mg, 98%) was obtained after washing with water (100 mL) and diethyl ether (100 mL) using vacuum suction filtration. $^{31}\text{P}\{^1\text{H}\}$ NMR (CD_2Cl_2): $\delta_{\text{P}} = 20.0$ ppm (s, $^1J_{\text{Pt-P}} = 3117$ Hz); ^1H NMR (CD_2Cl_2): $\delta_{\text{H}} = 2.08$ (br s, 4 H; 2SCH_2), 7.06–7.79 (m, 18 H; $2\text{C}_6\text{H}_4\text{C}_6\text{H}_5$), 7.06–7.79 ppm (m, 60 H; $12\text{C}_6\text{H}_5$); ESI-MS ($\text{MeOH}/\text{H}_2\text{O}$): m/z (%): 946 ($[\text{M}]^{2+}$, 100); elemental analysis: calcd (%) for $\text{Pt}_2\text{S}_2\text{C}_{100}\text{H}_{82}\text{P}_6\text{F}_{12}\text{O}_2$ (2183.83): C 55.00, H 3.78, S 2.94; found (%): C 54.89, H 3.17, S 2.56.

[Pt₂(μ-SCH₂C₆H₅)₂(dppp)₂](PF₆)₂ (8a). Benzyl bromide (40.0 μL, 57.5 mg, 0.336 mmol, 9 equiv.) was added to a bright yellow solution of **5** (49.5 mg, 0.039 mmol) in methanol (18 mL). The mixture was left to stir overnight until the reaction reached completion (ESI-MS ($\text{MeOH-H}_2\text{O}$): m/z (%): 730.2 (100, $[\text{M}]^{2+}$), 1540.9 (36, $[\text{M}]^{2+}\text{Br}^-$)). Excess NH_4PF_6 (20.0 mg, 0.123 mmol) was then added to the pale yellow solution. Deionized water (40 mL) was used to induce precipitation. Pale yellow powder of **8a** (55.1 mg, 81%) was obtained by washing with deionized water (100 mL) and diethyl ether (100 mL) using vacuum suction filtration. $^{31}\text{P}\{^1\text{H}\}$ NMR (CD_2Cl_2): $\delta_{\text{P}} = -0.7$ ppm (s, $^1J_{\text{Pt-P}} = 2733$ Hz); ^1H NMR (CD_2Cl_2): $\delta_{\text{H}} = 1.95$ (br s, 4 H; 2SCH_2), 2.90 (br s, 8 H; $2\text{PC}_3\text{H}_6\text{P}$), 3.35 (br s, 4 H; $2\text{PC}_3\text{H}_6\text{P}$), 6.44–6.46 (d, $J = 6.2$ Hz, 4 H; $2\text{CH}_2\text{C}_6\text{H}_5$), 6.98–7.05 (m, 6 H; $2\text{CH}_2\text{C}_6\text{H}_5$), 7.29–7.76 ppm (m, 40 H; $8\text{C}_6\text{H}_5$); ESI-MS ($\text{MeOH-H}_2\text{O}$): m/z (%): 730.5 ($[\text{M}]^{2+}$, 100), 1606.0 (15, $[\text{M}]^{2+}[\text{PF}_6]^-$); elemental analysis: calcd (%) for $\text{Pt}_2\text{S}_2\text{C}_{68}\text{H}_{66}\text{P}_6\text{F}_{12}$ (1751.36): C 46.63, H 3.80, S 3.66; found (%): C 46.99, H 3.85, S 3.23. Pale yellow crystals of $[\text{Pt}_2(\mu\text{-SCH}_2\text{C}_6\text{H}_5)_2(\text{dppp})_2](\text{PF}_6)_2$ suitable for X-ray crystallographic analysis were obtained from dichloromethane–methanol.

[Pt₂(μ-SCH₂CHCH₂)₂(dppp)₂](PF₆)₂ (8b**).** Allyl bromide (40.0 μL, 55.9 mg, 0.462 mmol, 11 equiv.) was added to a bright yellow solution of **5** (54.7 mg, 0.043 mmol) in methanol (18 mL). The mixture was stirred for 5 h until the reaction reached completion (ESI-MS (MeOH–H₂O): *m/z* (%): 680.2 (100, [M]²⁺), 1439.7 (35, [M]²⁺Br⁻)). Excess NH₄PF₆ (20.0 mg, 0.123 mmol) was then added, resulting in a light yellow suspension. Deionized water (40 mL) was used to complete precipitation. Pale yellow powder of **8b** (56.3 mg, 80%) was obtained by washing with deionized water (100 mL) and diethyl ether (100 mL) using vacuum suction filtration. ³¹P{¹H} NMR (CD₂Cl₂): δ_P = 0.7 ppm (s, ¹J_{Pt-P} = 2726 Hz); ¹H NMR (CD₂Cl₂): δ_H = 1.96 (br m, 4 H; 2SCH₂), 2.83–2.95 (br m, 12 H; 2PC₃H₆P), 4.64 (m, 2 H; 2CHCH_aH_b), 4.74 (m, 2 H; 2CHCH_aH_b), 4.79 (m, 2 H; 2SCH₂CH), 7.35–7.76 ppm (m, 40 H; 8C₆H₅); ESI-MS (MeOH–H₂O): *m/z* (%): 680 ([M]²⁺,

100), 1505 ([M]²⁺[PF₆]⁻, 55); elemental analysis: calcd (%) for Pt₂S₂C₆₀H₆₂P₆F₁₂ (1651.25): C 43.64, H 3.78, S 3.88; found (%): C 43.29, H 3.55, S 3.32.

[Pt₂(μ-SCH₂CN)₂(dppp)₂](PF₆)₂ (8c**).** A procedure similar to the above was employed. Bromoacetonitrile (40.0 μL, 68.9 mg, 0.574 mmol, 15 equiv.) was added into a bright yellow solution of **5** (47.1 mg, 0.037 mmol) in methanol (20 mL). The mixture was stirred for 2 h followed by the addition of excess NH₄PF₆ (20.0 mg, 0.123 mmol), resulting in a light yellow suspension. Deionized water (40 mL) was used to complete precipitation. Pale yellow powder of **8c** (42.9 mg, 71%) was obtained by washing with deionized water (100 mL) and diethyl ether (100 mL) using vacuum suction filtration. ³¹P{¹H} NMR (CD₂Cl₂): δ_P = 0.8 ppm (s, ¹J_{Pt-P} = 2775 Hz); ¹H NMR (CD₂Cl₂): δ_H = 2.04 (br m,

Table 3 Selected bond lengths (Å) and angles (°) for complexes **3a**, **3b**, **2a**, **8a** and **3e**

[Pt ₂ (μ-S)(μ-SCH ₂ CH ₂ CN)(PPh ₃) ₄](PF ₆) (3a)							
Pt(2)–P(3)	2.2884(19)	Pt(2)–S(1)	2.3525(18)	Pt(1)–S(1)	2.3371(16)	S(1)–C(1)	1.882(13)
Pt(2)–P(4)	2.2981(16)	Pt(2)–S(2)	2.345(5)	Pt(1)–S(2)	2.388(5)		
Pt(1)–S(1)–Pt(2)	89.82(6)	P(1)–Pt(1)–P(2)	98.12(5)	P(2)–Pt(1)–S(1)	168.17(6)	C(1)–S(1)–Pt(2)	101.6(4)
Pt(1)–S(2)–Pt(2)	88.78(18)	P(1)–Pt(1)–S(1)	93.62(6)	P(2)–Pt(1)–S(2)	171.61(12)	θ ^a	144
S(1)–Pt(1)–S(2)	84.28(12)	P(1)–Pt(1)–S(2)	171.61(12)	C(1)–S(1)–Pt(1)	102.2(4)		
[Pt ₂ (μ-S)(μ-SC ₂ H ₄ CO ₂ CH ₂ CH ₃)(PPh ₃) ₄](PF ₆) (3b)							
Pt(1)–P(1)	2.3002(15)	Pt(1)–S(1)	2.3458(14)	Pt(2)–S(1)	2.3312(14)	S(1)–C(1)	1.821(11)
Pt(1)–P(2)	2.2794(14)	Pt(1)–S(1A)	2.3313(14)				
Pt(1)–S(1)–Pt(2)	95.70(5)	P(1)–Pt(1)–S(1)	87.32(5)	P(2)–Pt(1)–S(2)	91.30(5)	θ ^a	157
S(1)–Pt(1)–S(2)	81.59(6)	P(1)–Pt(1)–S(2)	168.86(5)	C(1)–S(1)–Pt(1)	109.2(3)		
P(1)–Pt(1)–P(2)	99.76(5)	P(2)–Pt(1)–S(1)	172.79(5)	C(1)–S(1)–Pt(2)	103.3(4)		
[Pt ₂ (μ-SC ₁₀ H ₁₀ N) ₂ (PPh ₃) ₄](PF ₆) ₂ (2a)							
Pt(1)–P(1)	2.2929(13)	Pt(1)–S(1)	2.3498(13)	Pt(2)–S(1)	2.3689(12)	S(1)–C(1)	1.830(6)
Pt(1)–P(2)	2.3105(15)	Pt(1)–S(2)	2.3812(12)	Pt(2)–S(2)	2.3533(12)	S(2)–C(11)	1.839(6)
Pt(1)–S(1)–Pt(2)	90.42(5)	P(1)–Pt(1)–P(2)	97.69(5)	C(1)–S(1)–Pt(1)	103.5(2)	θ ^a	140
Pt(1)–S(2)–Pt(2)	90.04(4)	P(1)–Pt(1)–S(1)	94.18(5)	C(1)–S(1)–Pt(2)	109.20(19)		
S(1)–Pt(1)–S(2)	81.89(4)	P(1)–Pt(1)–S(2)	175.43(5)				
[Pt ₂ (μ-SCH ₂ C ₆ H ₅) ₂ (dppp) ₂](PF ₆) ₂ (8a)							
Pt(1)–P(1)	2.286(3)	Pt(1)–S(1)	2.370(3)	Pt(2)–S(1)	2.361(3)	S(1)–C(1)	1.836(13)
Pt(1)–P(2)	2.289(3)	Pt(1)–S(2)	2.372(3)	Pt(2)–S(2)	2.376(3)	S(2)–C(8)	1.843(11)
Pt(1)–S(1)–Pt(2)	89.58(10)	P(1)–Pt(1)–P(2)	90.37(11)	C(1)–S(1)–Pt(1)	108.2(5)	θ ^a	141
Pt(1)–S(2)–Pt(2)	89.18(9)	P(1)–Pt(1)–S(1)	92.51(10)	C(1)–S(1)–Pt(2)	105.5(4)		
S(1)–Pt(1)–S(2)	83.50(9)	P(1)–Pt(1)–S(2)	170.88(10)				
[Pt ₂ (μ-S)(μ-SCH ₂ C ₆ H ₅)(PPh ₃) ₄](PF ₆) (3e)							
Pt(1)–P(1)	2.3011(14)	Pt(1)–S(1)	2.3667(13)	Pt(2)–S(1)	2.3594(13)	S(1)–C(1)	1.850(6)
Pt(1)–P(2)	2.2671(13)	Pt(1)–S(2)	2.3209(13)	Pt(2)–S(2)	2.3363(13)		
Pt(1)–S(1)–Pt(2)	89.96(4)	P(1)–Pt(1)–P(2)	98.71(5)	P(2)–Pt(1)–S(1)	172.61(5)	C(1)–S(1)–Pt(2)	105.0(2)
Pt(1)–S(2)–Pt(2)	91.66(5)	P(1)–Pt(1)–S(1)	87.69(5)	P(2)–Pt(1)–S(2)	92.30(5)	θ ^a	140
S(1)–Pt(1)–S(2)	81.45(5)	P(1)–Pt(1)–S(2)	168.81(5)	C(1)–S(1)–Pt(1)	100.13(19)		

^a θ = Dihedral angle between the two PtS₂ planes.

Table 4 Crystallographic data for complexes **3a**, **3b**, **2a**, **8a** and **3e**

Complex	3a	3b	2a ·1.5CH ₂ Cl ₂ ·CH ₃ OH	8a ·4CH ₂ Cl ₂	3e ·2CH ₂ Cl ₂ ·2CH ₃ OH
Formula	C ₇₅ H ₆₄ F ₆ NP ₃ Pt ₂ S ₂	C ₇₇ H ₆₉ F ₆ O ₂ P ₃ Pt ₂ S ₂	C _{94.5} H ₈₇ Cl ₃ F ₁₂ N ₂ OP ₆ Pt ₂ S ₂	C ₇₂ H ₇₄ Cl ₈ F ₁₂ P ₆ Pt ₂ S ₂	C ₈₃ H ₇₉ Cl ₄ F ₆ O ₂ P ₃ Pt ₂ S ₂
<i>M</i>	1702.42	1749.47	2241.13	2091.03	1981.41
Crystal system	Monoclinic	Monoclinic	Triclinic	Triclinic	Triclinic
Space group	<i>P</i> 2(1)/ <i>c</i>	<i>C</i> 2/ <i>c</i>	<i>P</i> $\bar{1}$	<i>P</i> $\bar{1}$	<i>P</i> $\bar{1}$
<i>a</i> /Å	23.038(3)	17.5679(16)	13.1226(5)	13.5578(11)	13.5370(11)
<i>b</i> /Å	12.9432(17)	19.0008(16)	17.2989(7)	24.083(2)	14.0622(12)
<i>c</i> /Å	23.952(3)	21.5327(19)	21.3799(8)	27.457(2)	24.080(2)
<i>a</i> /°	90	90	89.893(10)	112.135(2)	81.118(2)
<i>β</i> /°	110.173(3)	90.508(3)	87.216(10)	101.057(2)	85.273(2)
<i>γ</i> /°	90	90	72.929(10)	94.877(2)	61.710(2)
<i>V</i> /Å ³	4465.0(5)	7187.4(11)	4633.7(3)	8027.4(11)	3987.7(6)
<i>Z</i>	4	4	2	4	2
ρ_{calcd} /g cm ⁻³	1.687	1.617	1.606	1.730	1.650
μ /mm ⁻¹	4.412	4.119	3.323	3.988	3.853
Temperature/K	223(2)	223(2)	183(2)	223(2)	223(2)
Reflections measured	46 800	24 358	61 431	105 953	51 960
Independent reflections	15 395	8243	21 244	36 850	18 308
<i>R</i> _{int}	0.0584	0.0574	0.0365	0.0897	0.0486
Parameters	865	448	1117	1864	949
<i>R</i> (<i>F</i> , <i>F</i> ² > 2σ)	0.0449	0.0435	0.044	0.082	0.0475
<i>R</i> _w (<i>F</i> ² , all data)	0.1127	0.1244	0.1336	0.2457	0.1265
Goodness of fit on <i>F</i> ²	0.969	0.985	1.075	1.050	1.043
Max., min. electron density/e Å ⁻³	1.781, -0.846	2.377, -0.593	2.943, -1.384	5.711, -2.565	3.732, -1.801

4 H; 2SCH₂), 2.54–3.01 (br m, 12 H; 2PC₃H₆P), 7.12–7.51 ppm (m, 40 H; 8C₆H₅); ESI-MS (MeOH–H₂O): *m/z* (%): 679 ([M]²⁺, 100), 1503 ([M]²⁺[PF₆]⁻, 70); elemental analysis: calcd (%) for Pt₂S₂C₅₈H₅₆N₂P₆F₁₂ (1649.19): C 42.24, H 3.42, N 1.70, S 3.89; found (%): C 42.42, H 3.71, N 1.16, S 3.84.

X-Ray crystal structure determination and refinement†

The selected bond lengths and angles for complexes **3a**, **3b**, **2a**, **8a** and **3e** are given in Table 3. All measurements were made on a Bruker AXS SMART APEX diffractometer equipped with a CCD area detector by using Mo-K α radiation ($\lambda = 0.71073$ Å). The software SMART²¹ was used for the collection of data frames, for indexing reflections, and to determine lattice parameters; SAINT²¹ was used for the integration of the intensity of the reflections and for scaling; SADABS²² was used for empirical absorption correction; and SHELXTL²³ was used for space group and structure determination, refinements, graphics, and structure reporting. The structure was refined by full-matrix least squares on *F*² with anisotropic thermal parameters for non-hydrogen atoms. A summary of crystallographic parameters for the data collections and refinements is given in Table 4.

For **3a**, the –CH₂CH₂CN group is switching positions (60 : 40) over the two sulfur atoms, causing disorder in the crystal packing. For **3b**, the –C₂H₄CO₂CH₂CH₃ chain has half occupancy in the asymmetric unit, which is the result of the switching of positions of the ester chain over the two sulfur atoms, and hence causes disorder. For **2a**, there are one and a half dichloromethanes and one molecule of methanol in the asymmetrical unit in addition to one titled cation and two PF₆⁻ anions. For complex **8a**, there are two titled cations, four PF₆⁻ anions (three complete ones and two half ones) and eight dichloromethane molecules (two of which are disordered) in the asymmetrical unit. For complex **3e**, there are

one titled cation and one PF₆⁻ anion in the asymmetrical unit. There are also two dichloromethane and two methanol solvent molecules. Restraints were applied in the refinement of **3a**, **3b** and **8a**. Restraints to the bond lengths and thermal parameters of the atoms were used for atoms involved in disorder and in structures for which the data quality needs to be improved. Upon application of restraints, the bond distances and thermal parameters became better and the *R* values were not increased.

Acknowledgements

We acknowledge the National University of Singapore for financial support and S. H. Chong thanks NUS for a Kiang Ai Kim Graduate Research Scholarship. We are grateful to L. L. Koh and G. K. Tan for assistance in the X-ray single-crystal crystallographic data collection and analyses.

References

- S. W. A. Fong and T. S. A. Hor, *J. Chem. Soc., Dalton Trans.*, 1999, 639.
- (a) S. H. Chong, L. L. Koh, W. Henderson and T. S. A. Hor, *Chem.–Asian J.*, 2006, **1**, 264; (b) P. González-Duarte, A. Lledós and R. Mas-Ballesté, *Eur. J. Inorg. Chem.*, 2004, 3585.
- (a) R. Mas-Ballesté, M. Capdevila, P. A. Champkin, W. Clegg, R. A. Coxall, A. Lledós, C. Mégret and P. González-Duarte, *Inorg. Chem.*, 2002, **41**, 3218; (b) M. Zhou, C. F. Lam, K. F. Mok, P.-H. Leung and T. S. A. Hor, *J. Organomet. Chem.*, 1994, **476**, C32.
- S. H. Chong, D. J. Young and T. S. A. Hor, *J. Organomet. Chem.*, 2006, **691**, 349.
- R. Ugo, G. La Monica, S. Cenini, A. Segre and F. Conti, *J. Chem. Soc. A*, 1971, 522.
- W. Henderson, S. H. Chong and T. S. A. Hor, *Inorg. Chim. Acta*, 2006, **359**, 3440.
- S. H. Chong, A. Tjindrawan and T. S. A. Hor, *J. Mol. Catal. A: Chem.*, 2003, **204–205**, 267.
- (a) S.-W. A. Fong, W. T. Yap, J. J. Vittal, T. S. A. Hor, W. Henderson, A. G. Oliver and C. E. F. Rickard, *J. Chem. Soc., Dalton Trans.*, 2001,

- 1986; (b) S.-W. A. Fong, J. J. Vittal, W. Henderson, T. S. A. Hor, A. G. Oliver and C. E. F. Rickard, *Chem. Commun.*, 2001, 421.
- 9 R. Mas-Ballesté, G. Aullón, P. A. Champkin, W. Clegg, C. Mégret, P. González-Duarte and A. Lledós, *Chem.–Eur. J.*, 2003, **9**, 5023.
- 10 J. S. L. Yeo, J. J. Vittal, W. Henderson and T. S. A. Hor, *J. Chem. Soc., Dalton Trans.*, 2002, 328.
- 11 H. Li, G. B. Carpenter and D. A. Sweigart, *Organometallics*, 2000, **19**, 1823.
- 12 (a) S.-W. A. Fong, T. S. A. Hor, S. M. Devoy, B. A. Waugh, B. K. Nicholson and W. Henderson, *Inorg. Chim. Acta*, 2004, **357**, 2081; (b) S.-W. A. Fong, T. S. A. Hor, J. J. Vittal, W. Henderson and S. Cramp, *Inorg. Chim. Acta*, 2004, **357**, 1152.
- 13 S. Jeram, W. Henderson, B. K. Nicholson and T. S. A. Hor, *J. Organomet. Chem.*, 2006, **691**, 2827.
- 14 F. Novio, R. Mas-Ballesté, I. Gallardo, P. González-Duarte, A. Lledós and N. Vila, *Dalton Trans.*, 2005, 2742.
- 15 (a) D. Seyferth, L.-C. Song and R. S. Henderson, *J. Am. Chem. Soc.*, 1981, **103**, 5103; (b) D. Seyferth and G. B. Womack, *J. Am. Chem. Soc.*, 1982, **104**, 6839.
- 16 (a) S. M. Aucott, D. Duerden, Y. Li, A. M. Z. Slawin and J. D. Woollins, *Chem.–Eur. J.*, 2006, **12**, 5495; (b) A. Singhal, V. K. Jain, A. Klein, M. Niemeyer and W. Kaim, *Inorg. Chim. Acta*, 2004, **357**, 2134; (c) E. W. Abel, N. A. Cooley, K. Kite, K. G. Orrell and V. Sik, *Polyhedron*, 1987, **6**, 1261.
- 17 (a) P. S. Braterman and V. A. Wilson, *J. Organomet. Chem.*, 1971, **31**, 123; (b) A. Singhal, V. K. Jain, B. Varghese and E. R. T. Tiekink, *Inorg. Chim. Acta*, 1999, **285**, 190.
- 18 (a) J. Ruiz, C. Vicente, V. Rodríguez and G. López, *Polyhedron*, 1998, **17**, 1503; (b) H. C. Clark, V. K. Jain and G. S. Rao, *J. Organomet. Chem.*, 1985, **279**, 181.
- 19 S. Dey, V. K. Jain, S. Chaudhury, A. Knoedler, F. Lissner and W. Kaim, *J. Chem. Soc., Dalton Trans.*, 2001, 723.
- 20 (a) A. Mendía, E. Cerrada, F. J. Arnáiz and M. Laguna, *Dalton Trans.*, 2006, 609; (b) R. Miao, G. Yang, Y. Miao, Y. Mei, J. Hong, C. Zhao and L. Zhu, *Rapid Commun. Mass Spectrom.*, 2005, **19**, 1031; (c) H. Wei, Q. Liu, J. Lin, P. Jiang and Z. Guo, *Inorg. Chem. Commun.*, 2004, **7**, 792; (d) U. Bierbach, T. W. Hambley and N. Farrell, *Inorg. Chem.*, 1998, **37**, 708; (e) L. R. Kelland, S. J. Clarke and M. J. McKeage, *Platinum Met. Rev.*, 1992, **36**, 178; (f) K. A. Mitchell and C. M. Jensen, *Inorg. Chem.*, 1995, **34**, 4441; (g) I. H. Krakoff, *Cancer Treat. Rep.*, 1979, **63**, 1523; (h) M. Dentre, F. C. Luft, N. M. Yum, S. D. Williams and L. H. Einhorn, *Cancer*, 1978, **41**, 1274.
- 21 *SMART & SAINT Software Reference Manuals, Version 4.0*, Siemens Energy & Automation, Inc., Analytical Instrumentation, Madison, WI, USA, 1996.
- 22 G. M. Sheldrick, *SADABS, a software for empirical adsorption correction*, University of Göttingen, Göttingen, Germany, 1993.
- 23 G. M. Sheldrick, *SHELXTL, VERSION 5.03*, Siemens Energy & Automation, Inc., Analytical Instrumentation, Madison, WI, USA, 1996.